Phytochemistry 88 (2013) 34–42

Contents lists available at SciVerse ScienceDirect

Phytochemistry

journal homepage: www.elsevier.com/locate/phytochem

LC–MS/APCI identification of glucoside esters and diesters of astaxanthin from the snow alga *Chlamydomonas nivalis* including their optical stereoisomers

Tomáš Řezanka [a,*], Linda Nedbalová [b,c], Irena Kolouchová [d], Karel Sigler [a]

[a] Institute of Microbiology, Academy of Sciences of the Czech Republic, Vídeňská 1083, 142 20 Prague, Czech Republic
[b] Charles University in Prague, Faculty of Science, Department of Ecology, Viničná 7, 128 44 Prague 2, Czech Republic
[c] Institute of Botany, Academy of Sciences of the Czech Republic, Dukelská 135, 379 82 Třeboň, Czech Republic
[d] Department of Biotechnology, Institute of Chemical Technology Prague, Technická 5, 166 28 Prague, Czech Republic

ARTICLE INFO

Article history:
Received 17 September 2012
Received in revised form 7 January 2013
Available online 8 February 2013

Keywords:
Chlamydomonas nivalis
Snow alga
Austrian Alps
Bulgarian Pirin
Slovak High Tatra Mountains
Astaxanthin glucoside esters
Astaxanthin esters
LC–MS/APCI
Chiral HPLC
Optical isomers–enantiomers

ABSTRACT

HPLC methods (LC–MS/APCI and chiral HPLC) were used for the identification of astaxanthin derivatives from the red snow alga *Chlamydomonas nivalis* collected in Austrian Alps, Slovak High Tatra Mountains and Bulgarian Pirin. We observed a striking difference in the composition of astaxanthin optical isomers in *C. nivalis* collected in geographically distinct regions. Furthermore, algae from the Pirin Mountains differed in the dominance of astaxanthin diglucoside diesters, suggesting an alternative strategy to enhance cell viability at low temperatures.

1. Introduction

Snow algae that inhabit alpine localities in all continents as well as Polar Regions represent an ecologically and physiologically highly specialized group of algal species. Typical cryosestic and exclusively cryophilic green algae are represented particularly by several species of *Chlamydomonas* and *Chloromonas* (Chlorophyta, Chlamydomonadales) with complicated life cycles involving flagellated vegetative cells and immotile resting spores or cysts with thick walls and large amounts of carotenoids and lipid reserves (Hoham and Duval, 2001).

Numerous snow algae, including the most common *Chlamydomonas nivalis* (Hoham and Duval, 2001), still need taxonomic revision. It is probable that the reddish coloration of snow at alpine sites is caused by more species with similar immotile cells, as it was already observed in Antarctica (Ling, 1996; Fujii et al., 2010). The typical red spherical cells without flagella contain high amounts of astaxanthin that protects cells from UV-damage and potential photoinhibition (Bidigare et al., 1993), enables the transfer of excitation energy to chlorophyll *a* (Droop, 1955; Goodwin, 1980), and is also an effective antioxidant (Tinkler et al., 1994). Mature resting stages of *C. nivalis* may contain 20–30 times more astaxanthin than chlorophyll *a* (Muller et al., 1998; Remias et al., 2005). Astaxanthin and its esters are concentrated in cytoplasmic lipid droplets (Gorton and Vogelman, 2003). Esterification of astaxanthin allows efficient pigment concentration in cytoplasm, and a contrasting proportion of mono- and diesters was recorded in samples from different geographic regions (Bidigare et al., 1993). In addition, the water content in cells is reduced when astaxanthin concentration is high, reducing ice crystal formation (Hoham, 1992).

The only useful method for analysis of carotenoids is high-performance liquid chromatography–mass spectrometry (LC–MS). Several LC–MS methods have been reported for carotenoid analysis; APCI (atmospheric-pressure chemical ionization) is the most widely used ionization technique, which shows high sensitivity in the analysis of not only free carotenoids but also their esters and glycosides (Rivera and Canela-Garayoa, 2012).

Most of the data published so far describe only the identification of pseudomolecular ions (Takaichi et al., 2003), usually in a high-resolution mode (Burgess et al., 1999; Yokoyama et al., 1995b). Several papers dealt with the analysis of acyls. The first of these studies (Breithaupt et al., 2002) describes the pseudomolecular ion $[M+H]^+$ and other ions which we also identified and describe, i.e. $[M+H-H_2O]^+$, $[M+H-FA_1]^+$, $[M+H-FA_1-H_2O]^+$,

* Corresponding author. Tel.: +420 241 062 300; fax: +420 241 062 347.
E-mail address: rezanka@biomed.cas.cz (T. Řezanka).

0031-9422/$ - see front matter © 2013 Elsevier Ltd. All rights reserved.
http://dx.doi.org/10.1016/j.phytochem.2013.01.003

$[M+H-FA_1-FA_2]^+$, $[M+H-FA_1-FA_2-H_2O]^+$, where FA is fatty acid. Another study identified astaxanthin esters, including both monoesters and diesters, in aquatic organisms (Breithaupt, 2004). Among the metabolites in phytoplankton described by Frassanito et al. (2005, 2006) only adonirubin among the many xanthophylls (i.e. carotenoids containing a polar group, e.g. hydroxyl(s), etc.) present was esterified by two different polyenoic fatty acids (18:4 and 20:5). Two other studies (Schweiggert et al., 2005; Miao et al., 2006) devoted to carotenoid esters in red pepper pods and in mandarin essential oil also made use of tandem MS (MS^n) and identified the appropriate ions, i.e. $[M+H]^+$ and $[M+H-FA_1]^+$. Using tandem MS (MS^n), and even better LC–MS^n allows the analyst to increase analysis selectivity and specificity, facilitating identification of coeluted carotenoids or structural isomers.

Astaxanthin exists as two enantiomers (3*R*,3′*R* and 3*S*,3′*S*) and a meso form (3*R*,3′*S*; 3*S*,3′*R*). In nature it occurs as the nearly pure 3*S*,3′*S* isomer predominantly in photosynthetic organisms such as the green alga *Haematococcus pluvialis* (Renstrom et al., 1981c; Lorenz and Cysensky, 2000), or was identified from the red flower petals of *Adonis annua*. It occurs both as a diester (64% of total carotenoid) and as a monoester (11%) (Renstrom et al., 1981a). The natural bloom of *Euglena sanguinea* also contains diesters of (3*S*,3′*S*)-astaxanthin (75%), as major compounds (Grung and Liaaen-Jensen, 1993).

An almost pure 3*R*,3′*R* isomer was identified in the red yeast *Phaffia rhodozyma* (Andrenes and Starr, 1976; Andrenes et al., 1976; Muller et al., 1980). Different ratios of astaxanthin optical isomers were found in different tissues of crustaceans, lobster eggs, shrimps, trout and salmon, indicating some selectivity in the tissue metabolism of the optical isomers of astaxanthin (Moretti et al., 2006; Ronneberg et al., 1980; Renstrom et al., 1981b).

Optical isomers can be separated after derivatization with a suitable reagent (e.g. (−)-camphanoyl chloride) and the resulting diastereoisomers can be easily resolved on an achiral phase column (Vecchi and Muller, 1979; Bonen et al., 2002; Coral-Hinostroza and Bjerkeng, 2002). An alternative method is direct HPLC analysis of underivatized astaxanthin on a chiral column that avoids various problems with derivatization (Maoka et al., 1985; Turujman, 1993; Abu-Lafi and Turujman, 1999; Grewe et al., 2007; Rezanka and Dembitsky, 1998).

The objective of the present study was to determine the chemical composition of the snow alga *C. nivalis* collected from high-altitude environments of Austrian Alps, Bulgarian Pirin and Slovak High Tatra Mountains with the aim of separating astaxanthin glycoside esters and astaxanthin esters and identifying their structures by means of LC–MS. Major and also minor astaxanthin derivatives were characterized in APCI positive ion mode by their specific fragmentation patterns, revealing a more complex profile than described so far. Further, HPLC analysis of free astaxanthin on a chiral column showed that the distribution of algal astaxanthin enantiomers from the Alps and High Tatra is different from the algal astaxanthins from the Pirin. This is the first comparative study of native astaxanthin esters by LC–MS/APCI and also of astaxanthin enantiomers from snow algae.

2. Results and discussion

2.1. Separation and identification of optical isomers–enantiomers

The MeOH extracts from the snow alga *C. nivalis* collected in Austria, Slovakia and Bulgaria were separately hydrolyzed, i.e. esters and glycosides of astaxanthin were transformed to a mixture of free optical isomers, which were further separated by chiral HPLC, see Fig. 1 and Table 1. In our case, all geometrical isomers of astaxanthins having at least one cis double bond were present in amounts below 1% of total astaxanthins and are therefore not included in the manuscript. The chromatogram of a natural mixture of all geometrical isomers of astaxantins is in Fig. 1S (Supplements) and ^1H NMR data are in Table 1S.

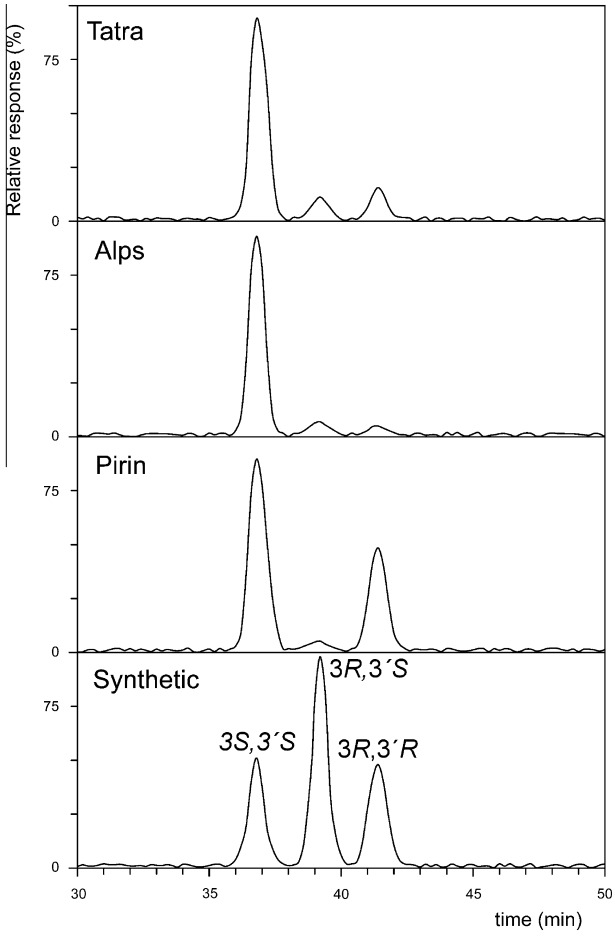

Fig. 1. Chiral HPLC of astaxanthin from different localities.

Table 1
Individual enantiomers of astaxanthins from the snow alga *Chlamydomonas nivalis* collected in Slovak Tatra, Austrian Alps and Bulgarian Pirin.

Isomer	Synthetic	Tatra	Alps	Pirin
3S,3′S	25.2	77.8	85.2	61.6
3S,3′R	47.5	9.3	8.7	4.8
3R,3′R	27.3	12.9	6.1	33.6

The Bulgarian snow alga contained predominantly a mixture of astaxanthins that possessed mostly the 3*R*,3′*R* and 3*S*,3′*S* astaxanthin isomers, and very little of the 3*R*,3′*S* isomer (meso-isomer). Chiral analysis see Fig. 1, of the Austrian and Slovakian snow alga revealed a high content of only the 3*S*,3′*S* isomer while a synthetic mixture (commercially available astaxanthin) gave the expected results, with approximately 1:2:1 (3*S*,3′*S*:3*R*,3′*S*:3*R*,3′*R*) ratio of the individual isomers. The structure of all three isomers of astaxanthin has been proven as a high-resolution mass spectrometry by Orbitrap, see Fig. 2S in Supplements and our by measuring of the circular dichroism described in our already published paper (Rezanka and Dembitsky, 1998).

So far only marine organisms such as lobster, shrimp, red crab, langostilla, etc. (Coral-Hinostroza and Bjerkeng, 2002), or salmon (Megdal et al., 2009) have been reported to contain a mixture of all three optical isomers, whereas photosynthesizing organisms such as *Adonis* or algae contain a nearly 100% pure 3*S*,3′*S*

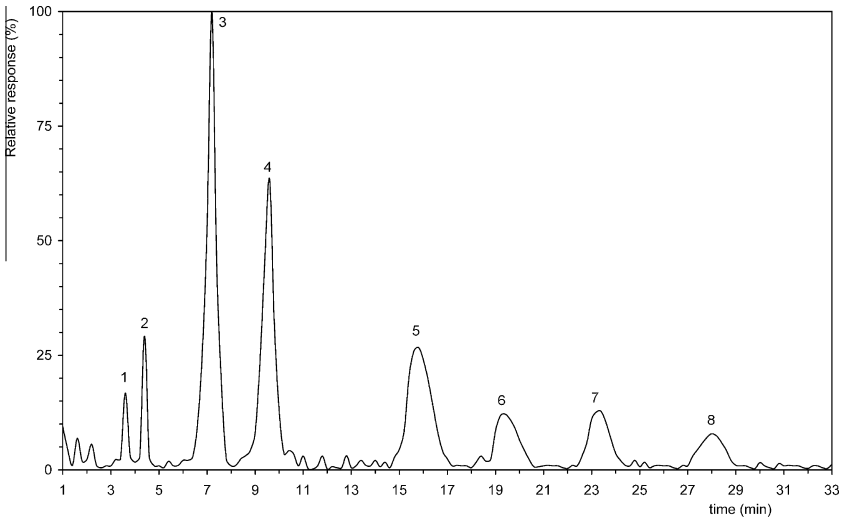

Fig. 2. Preparative HPLC of total extract of carotenoids from *Chlamydomonas nivalis* collected in Austrian Alps, Peak 1 (G-A-G), 2 (G-A), 3 (FA-G-A-G), 4 (FA-G-A-G-FA), 5 (xanthophylls), 6 (FA-A), 7 (FA-A-FA), and 8 (carotenoid hydrocarbons).

Table 2
Quantitative distribution of astaxanthin glucoside esters (FA-G-A-G) from the snow alga *Chlamydomonas nivalis* collected in Austrian Alps determined by LC–MS/APCI.

No	RT	Acid	%	$[M+H]^+$
1	11.17	16:4n3	6.9	989
2	11.26	18:5n3	3.9	1015
3	12.96	16:3n6	9.2	991
4	13.04	16:3n4	2.6	991
5	13.11	16:3n3	5.1	991
6	13.39	18:4n3	5.1	1017
7	13.72	22:6n3	4.5	1069
8	14.75	16:2n6	2.9	993
9	14.89	16:2n4	1.4	993
10	15.02	18:3n3	6.8	1019
11	15.34	20:4n6	2.8	1045
12	15.57	20:4n3	1.2	1045
13	16.54	14:0	1.0	969
14	16.79	16:1n7	5.4	995
15	16.96	16:1n9	1.2	995
16	17.24	18:2n6	4.7	1021
17	18.34	16:0	11.6	997
18	18.75	18:1n9	21.0	1023
19	18.84	18:1n7	1.7	1023
20	20.12	18:0	1.0	1025

enantiomer. On the other hand, yeast of the genus *Pfaffia* produces only 3*R*,3′*R* optical isomer (Andrenes and Starr, 1976).

Identification of a mixture of enantiomers in the alga collected in Pirin implies that either both enantiomers are biosynthesized or a racemization of one to the other takes place. The latter possibility seems to be less probable because the meso-isomer has not been found in any sizable amount.

Further, the MeOH extracts from all three snow algae were separately subjected to preparative normal phase HPLC, see Fig. 2. A total of eight peaks were separated and identified; two peaks contain free carotenoids (xanthophylls and carotenoid hydrocarbons) and the remaining six peaks are esters or glycosides of astaxanthin.

2.2. Positional isomers of fatty acids

The most abundant peak from the extract of Austrian algae in preparative HPLC is that with a retention time of 7.2 min. This fraction was identified as FA-G-A-G (where FA is fatty acid, G is glucose, and A is astaxanthin); its content is given in Table 2. We succeeded in separating not only compounds with different molecular masses but also positional isomers of fatty acids, i.e.

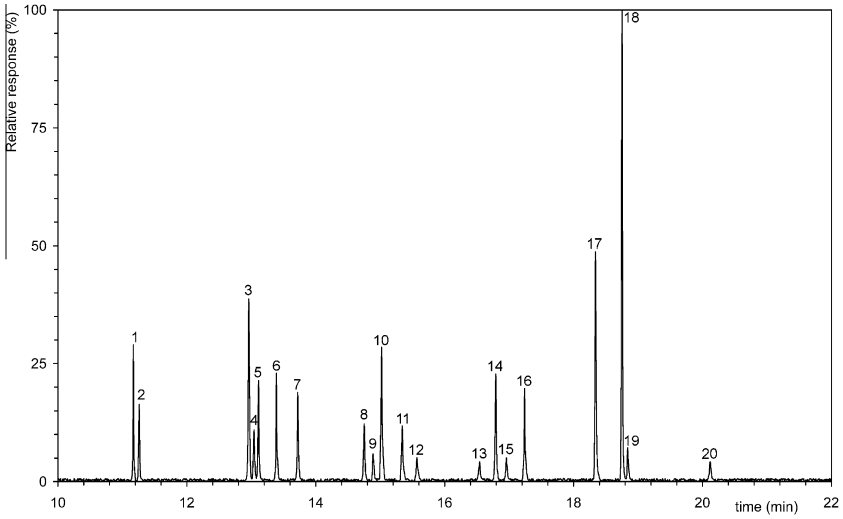

Fig. 3. LC–MS of fraction FA-G-A-G at 7.2 min, see Fig. 2.

compounds differing only in the position of the double bond in the acyl moiety, e.g. 18:1*n*-9-G-A-G and/or 18:1*n*-7-G-A-G (peaks No. 18 and 19). This is documented in Fig. 3 and Table 2S. A total of 20 molecular species of 6-*O*-acyl-diglucoside-astaxanthins were found. Complete information on the species is in the Supplements.

2.3. Different fractions of astaxanthins

Table 3 and Table 3S give the data obtained after RP-HPLC from fraction eluted at 23.4 min, i.e. 3,3′-diacyl-astaxanthin (FA-A-FA) which had the highest weight proportion in the Austrian alga, whereas in the Bulgarian alga it was the fraction FA-G-A-G-FA, as described previously (Rezanka et al., 2008). Complete information on the species is in the Supplements, see Table 4S. A total of 69 peaks were separated by LC–MS/APCI on narrow-bore columns connected in series (Fig. 4). By using MS/MS we succeeded in at least semiquantitatively identifying 105 molecular species. Substitution by any acyl chain does not modify the chromophore (Yamano et al., 2002; Yokoyama et al., 1995a, 1998; Giuffrida et al., 2006). All astaxanthin diesters exhibit very similar, if not identical, UV spectra (200–550 nm) (Yuan et al., 2002) and do not provide a clue for identification of the appropriate structures.

The components of both fractions were also analyzed after hydrolysis. Both fractions contained astaxanthin as the xanthophyll moiety and glucose was the only sugar, which was detected in the fraction of FA-G-A-G. The fatty acid composition (Table 4), determined by GC–MS, was qualitatively identical with the results obtained by APCI analysis. According to Dodds et al. (2005) and Lissitsyna et al. (2012) the responses of FID and MS used as a detector are similar. Hence, in terms of accuracy of analysis the quantification only by MS does not differ too much from the actual proportions of FAs. Moreover, one should take into account the biological nature of the samples. Due to variation in local climatic factors the habitats of snow algae are highly variable both in time and space. This results in a high seasonal variability in pigment content (Remias et al., 2005, 2010).

Table 4 illustrates a substantial difference between the quantitative compositions of FAs in the two types of compounds. The major FAs in FA-G-A-G esters are shorter FAs (in particular C16 and C18), oleic acid forming a quarter of all FAs. Interesting is the comparison of FA chain lengths, see lines in Table 4 bottom. Whereas in the sum of C16 the FA-G-A-G to FA-A-FA ratio is 4:3, with increasing chain length the ratio becomes more even and in the sum of C20 and C22 it is in fact inverted, i.e. ~1:2. On the other hand, UI (unsaturation index), which was calculated as the number of double bonds per 100 fatty acids (the percent abundance of each fatty acid × number of double bonds, summed for all fatty acids) is the same for both fractions although there are large differences in terms of chain lengths. The same is true for iodine values, see last line in the Table 4. In conclusion it can be stated that both fractions have probably the same fluidity in the membranes and contribute thus about equally to cell viability.

2.4. Fragmentation patterns

Optimum APCI conditions were established by using a previously described data (Rezanka et al., 2008). The fragmentation of the astaxanthin diester can be performed at two different voltage values. If the cone voltage was set at 30 V in the positive mode, all compounds exhibited strong $[M+H]^+$ peaks (data not shown) but no fragmentation was observed, whereas a higher cone voltage (70 V) gave rise to fragmentation and individual daughter ions can be used for identification of molecular species. LC–MS analysis at *m/z* 400–1600 of the extract using an APCI showed $[M+H]^+$ (pseudomolecular ions) for the peaks characteristic for astaxanthin diesters and allowed the attribution of their molecular weights. A

Table 3
Quantitative distribution of astaxanthin diesters (FA-A-FA) from the snow alga *Chlamydomonas nivalis* from Austrian Alps determined by LC–MS/APCI.

Peak	RT	Mol.	Spec.	%[a]	Ratio[b]	$[M+H]^+$
1	6.11	18:5	18:5	0.55		1109
2	6.21	18:5	16:4	0.71		1083
3	6.33	16:4	16:4	0.87		1057
4	6.68	22:6	18:5	0.58		1163
5	6.73	22:6	16:4	0.74		1137
6	6.83	18:5	18:4	0.61		1111
7	7.18	18:5	16:3	2.14	30	1085
		18:4	16:4		70	1085
8	7.31	16:4	16:3	1.53		1059
9	7.43	22:6	22:6	0.61		1217
10	7.54	22:6	18:4	0.65		1165
11	7.93	22:6	16:3	1.41		1139
12	8.12	20:4	18:5	0.63		1139
13	8.18	20:4	16:4	0.79		1113
14	8.36	18:5	18:3	1.38	40	1113
		18:4	18:4		60	1113
15	8.53	18:5	16:2	2.95	30	1087
		18:4	16:3		40	1087
		18:3	16:4		40	1087
16	8.68	16:4	16:2	3.01	60	1061
		16:3	16:3		40	1061
17	8.95	22:6	20:4	0.66		1193
18	9.12	22:6	18:3	0.73		1167
19	9.32	22:6	16:2	0.68		1141
20	9.44	20:4	18:4	0.69		1141
21	9.65	20:4	16:3	1.45		1115
22	9.85	18:5	18:2	1.36	50	1115
		18:4	18:3		50	1115
23	9.97	18:5	16:1	3.75	30	1089
		18:4	16:2		20	1089
		18:3	16:3		20	1089
		18:2	16:4		30	1089
24	10.15	18:5	14:0	0.40		1063
25	10.29	16:4	16:1	2.39	40	1063
		16:3	16:2		60	1063
26	10.61	16:4	14:0	0.56		1037
27	10.74	22:6	18:2	0.63		1169
28	10.79	22:6	16:1	0.79		1143
29	10.87	22:6	14:0	0.43		1117
30	10.95	20:4	20:4	0.71		1169
31	11.18	20:4	18:3	0.78		1143
32	11.31	20:4	16:2	0.73		1117
33	11.50	18:5	18:1	3.11	50	1117
		18:4	18:2		20	1117
		18:3	18:3		30	1117
34	11.66	18:5	16:0	5.76	20	1091
		18:4	16:1		20	1091
		18:3	16:2		15	1091
		18:2	16:3		15	1091
		18:1	16:4		30	1091
35	11.87	18:4	14:0	0.47		1065
36	12.02	16:4	16:0	3.45	25	1065
		16:3	16:1		35	1065
		16:2	16:2		40	1065
37	12.26	16:3	14:0	1.23		1039
38	12.39	22:6	18:1	1.63		1171
39	12.48	22:6	16:0	0.99		1145
40	12.64	20:4	18:2	0.67		1145
41	12.82	20:4	16:1	0.84		1119
42	12.97	20:4	14:0	0.48		1093
43	13.10	18:5	18:0	2.82	20	1119
		18:4	18:1		35	1119
		18:3	18:2		45	1119
44	13.29	18:4	16:0	5.60	15	1093
		18:3	16:1		25	1093
		18:2	16:2		15	1093
		18:1	16:3		35	1093
		18:0	16:4		15	1093
45	13.49	16:3	16:0	2.64	65	1067
		16:2	16:1		35	1067
46	13.60	18:3	14:0	0.55		1067
47	13.81	16:2	14:0	0.50		1041
48	14.07	22:6	18:0	0.43		1173

(*continued on next page*)

Table 3 (*continued*)

Peak	RT	Mol.	Spec.	%[a]	Ratio[b]	$[M+H]^+$
49	14.21	20:4	18:1	1.68		1147
50	14.34	20:4	16:0	1.03		1121
51	14.53	18:4	18:0	2.86	20	1121
		18:3	18:1		60	1121
		18:2	18:2		20	1121
52	14.76	18:3	16:0	4.85	15	1095
		18:2	16:1		15	1095
		18:1	16:2		55	1095
		18:0	16:3		15	1095
53	14.93	18:2	14:0	0.45		1069
54	15.03	16:2	16:0	2.02	50	1069
		16:1	16:1		50	1069
55	15.19	16:1	14:0	0.61		1043
56	15.33	14:0	14:0	0.25		1017
57	15.73	20:4	18:0	0.48		1149
58	16.02	18:3	18:0	2.20	35	1123
		18:2	18:1		65	1123
59	16.34	18:2	16:0	3.24	25	1097
		18:1	16:1		55	1097
		18:0	16:2		20	1097
60	16.53	18:1	14:0	1.45		1071
61	16.72	16:1	16:0	1.17		1071
62	16.89	16:0	14:0	0.81		1045
63	17.65	18:2	18:0	3.10	10	1125
		18:1	18:1		90	1125
64	17.98	18:1	16:0	2.61	75	1099
		18:0	16:1		25	1099
65	18.42	18:0	14:0	0.25		1073
66	18.56	16:0	16:0	1.36		1073
67	19.49	18:1	18:0	1.45		1127
68	19.95	18:0	16:0	0.81		1101
69	21.41	18:0	18:0	0.25		1129

[a] Abundance.

[b] The ratio of isomers, determined solely from the detector response to each one of the compounds and from the mass spectra of the respective astaxanthin glucoside esters.

Table 4
FA composition in FA-G-A-G and FA-A-FA fraction, see Fig. 2, determined by GC–MS in *Chlamydomonas nivalis* collected in Austrian Alps.

Acid	FA-G-A-G%	FA-A-FA%
14:0	1.00	6.40
16:0	10.57	10.80
16:1*n*-7	5.48	5.26
16:1*n*-9	1.08	1.84
16:2*n*-4	1.69	1.98
16:2*n*-6	2.54	2.63
16:3*n*-3	4.95	1.75
16:3*n*-4	2.34	0.62
16:3*n*-6	8.97	2.63
16:4*n*-3	7.04	5.41
18:0	0.97	7.62
18:1*n*-7	1.82	1.64
18:1*n*-9	20.53	9.64
18:2*n*-6	4.45	6.40
18:3*n*-3	6.96	5.21
18:4*n*-3	5.02	4.44
18:5*n*-3	4.08	5.27
20:4*n*-3	1.13	3.51
20:4*n*-6	2.55	6.10
22:6*n*-3	6.83	10.85
C14	1.00	6.40
C16	44.66	32.92
C18	43.83	40.22
C20 + 22	10.51	20.46
UI C16	55.70	103.54
UI C18	91.96	52.96
UI C20 + 22	92.61	83.82
Suma UI	240.27	240.32
Iodine value	195	203

similar situation has already been observed (Breithaupt, 2004). The following discussion of the APCI mass spectra of the astaxanthin diesters studied here includes probable assignments of fragmentation pathways for each compound analyzed.

2.4.1. Fragmentation of FA-A-FA fraction

Some fragmentation of the peak at 17.65 min (No. 63 in Fig. 5, 18:1-A-18:1 and 18:0-A-18:2) was evident with a fragmenter voltage of 70 V. The parent ion at *m/z* 1125 $[M+H]^+$ dissociates to ions (*m/z* 859 $[M+H-FA_1]^+$, identical in this case with $[M+H-FA_2]^+$, *m/z* 843 $[M+H-FA_1-H_2O]^+ = [M+H-FA_2-H_2O]^+$, and ions common to all astaxanthin diesters *m/z* 595 $[M+H-FA_1-FA_2]^+$; *m/z* 579 $[M+H-FA_1-FA_2-H_2O]^+$ and *m/z* 561 $[M+H-FA_1-FA_2-2xH_2O]^+$. Ions belonging to the minor positional isomer, see also Fig. 5, i.e. ions at *m/z* 857 $[M+H-18:0]^+$ and at *m/z* 841 $[M+H-18:0-H_2O]^+$ were identified. The other 105 compounds had very similar mass spectra. We illustrate this on the peak with retention time 13.29 min ($[M+H]^+$ at 1093 Da, peak 44), which is a mixture of five molecular species: 18:4-A-16:0, 18:3-A-16:1, 18:2-A-16:2, 18:1-A-16:3 and 18:0-A-16:4 (Fig. 6). Its semiquantitation was done by using a previously described method (Rezanka et al., 2009), which

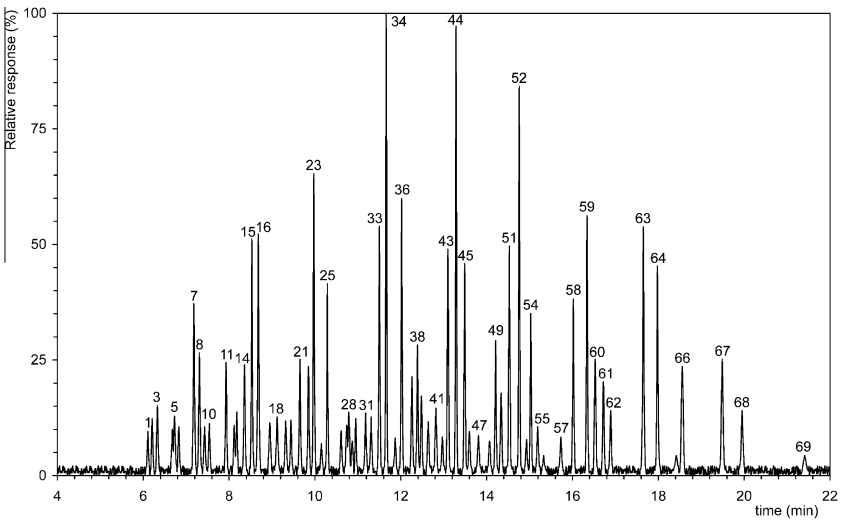

Fig. 4. LC–MS of fraction FA-A-FA at 23.4 min, see Fig. 2.

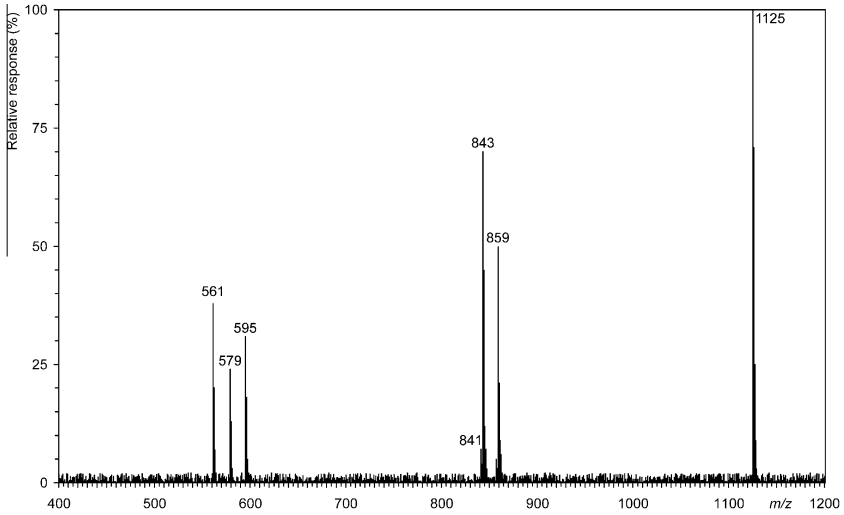

Fig. 5. Mass spectrum of a mixture of two molecular species – 18:1-A-18:1 and 18:2-A-18:0.

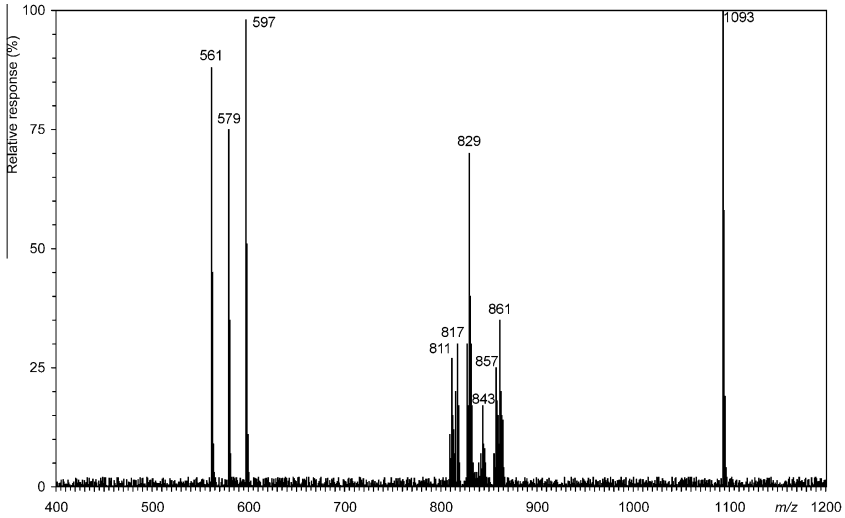

Fig. 6. Mass spectrum of a mixture of molecular species of 18:4-A-16:0, 18:3-A-16:1, 18:2-A-16:2, 18:1-A-16:3, and 18:0-A-16:4.

makes use of the abundance of $[M+H-FA_1]^+$ and/or $[M+H-FA_2]^+$ ions for determining peaks inseparable by HPLC. The results are documented in Table 3S. The chromatographic separation of compounds having the same molecular mass and differing in the degree of unsaturation of individual fatty acids (regioisomers), and of positional isomers of fatty acids in esters with astaxanthin was not successful. Compound 18:1*n*-9-A-18:1*n*-9 was synthesized for full confirmation of the results.

2.4.2. Fragmentation of FA-G-A-G and FA-G-A-G-FA fractions

Fragmentation of the peak 63 from the FA-G-A-G fraction showed ions at *m/z* 1185 $[M+H]^+$, *m/z* 1021 $[M-Glc]^+$, *m/z* 919 $[M-Acyl]^+$, *m/z* 757 $[M-Acyl-Glc]^+$, and *m/z* 595 $[M-Acyl-2xGlc]^+$, which were observed for molecular 18:1*n*-9-Glc-A-Glc species. Further fragmentation of these molecular species is mentioned below Tables 2 and 2S.

Although no differences in the spectra were observed between positional isomers, e.g. 18:1*n*-9-Glc-A-Glc and 18:1*n*-7-Glc-A-Glc, see also Fig. 3, these positional isomers could be separated chromatographically under given conditions and their content could thus be quantified.

The RP-HPLC fraction FA-G-A-G-FA obtained from preparative HPLC (at 9.6 min) is shown in Fig. 3S (Supplements). A total of 68 peaks were identified, see Table 4S (Supplements) which contained a minimum of 105 molecular species. Their quantification was performed similarly as in fraction FA-A-FA, i.e. on the basis of abundance of the ions $[M+H-FA_1]^+$, $[M+H-FA_2]^+$, $[M+H-Glc-FA_1]^+$ and $[M+H-Glc-FA_2]^+$. Our preceding paper has described in detail the mass spectral fragmentation of individual molecular species. A detailed description of the fragmentation including the *m/z* values of individual molecular species and corresponding ions is also given in Table 4S and in the paper by Rezanka et al. (2008). In the case of peaks containing isobaric compounds, i.e. compound FA-G-A-G s having the same molecular weight and differing only in the content of fatty acids, such as the peak 34 (retention time 21.34 min), the procedure was the same as in the identification of molecular species from fraction FA-A-FA.

The survival strategy of snow algae in cold climate, i.e. in polar and high altitude regions is dependent on the biosynthesis of specific components with multiple physiological functions. Carotenoids serve as passive photoprotectants (Gorton et al., 2001; Gorton and Vogelman, 2003) and also have antioxidant activity

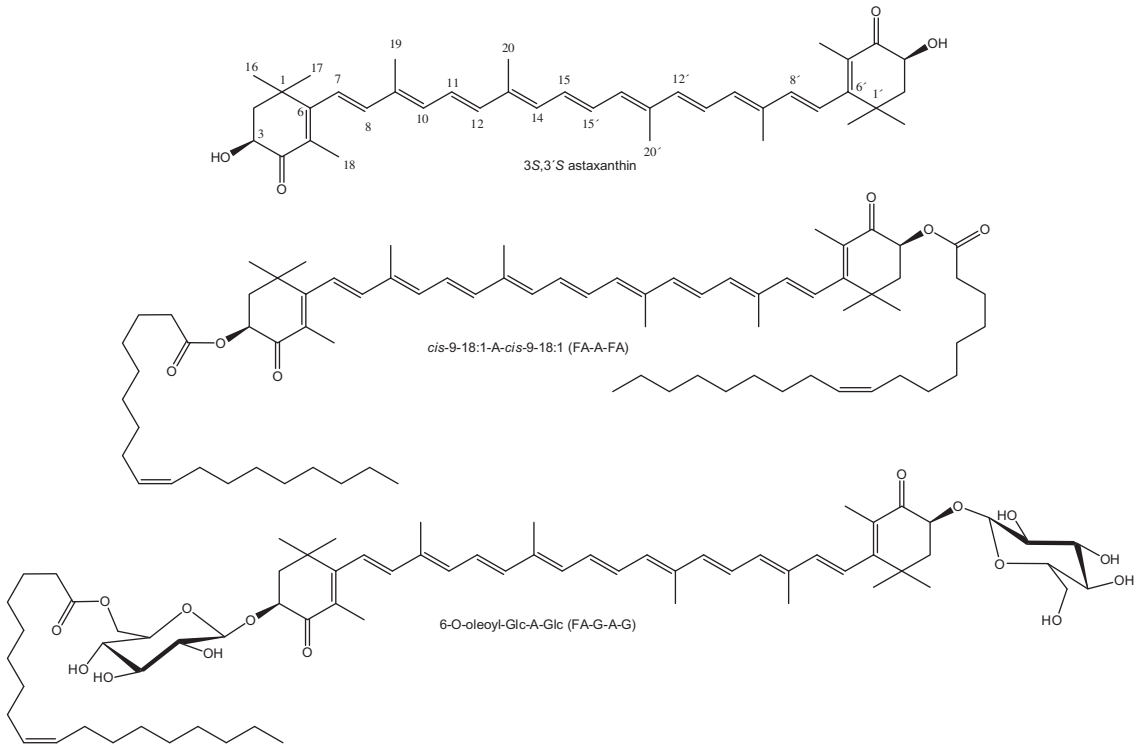

Fig. 7. Structures of astaxanthin, its ester and diglycoside ester.

(Kobayashi and Okada, 2000; Boussiba, 2000). They may act as multipurpose protective compounds against potentially damaging UV and VIS radiation. Derivatives of astaxanthin also exhibit cryoprotective effect and thus reduce the amount of cellular water and may decrease damage from ice crystals (Hoham, 1992). In addition, polyenoic fatty acids preserve the fluidity of membranes at extreme temperatures (Rezanka et al., 2008). Finally, carotenoids having bipolar, linear, and rigid structures may be responsible for general membrane stabilization (Ourisson et al., 1987; Yokoyama et al., 1996). Similar results were published for analogous structures such as thermozeaxanthins and thermocryptoxanthins from thermophilic bacteria (Yokoyama et al., 1995b, 1996). Further carotenoid glucoside esters, e.g. zeaxanthin mono- and diglucoside esters produced by *Thermus thermophilus* (Yokoyama et al., 1995a, 1996) showed that membrane-associated carotenoids in most cases are mono-cyclic or bis-cyclic, with one or two C-6 acylated glucosyl units involved with characteristic acyl groups (Yamano et al., 2002), which is also our case, see structures in Fig. 7.

3. Conclusion

In this section we would like to emphasize several points that follow from the above analyses. The first point refers to the high proportion of the astaxanthin 3*R*,3*R*′ enantiomer in the alga from Pirin. This may reflect either the biosynthesis of both enantiomers or their racemization. However, the latter possibility iTables less probable due to the negligible presence of the meso-form when compared with the synthetic astaxanthin. The second point concerns the different proportion of astaxanthin esters and glycosides in algae from Pirin and from Alps. The life conditions of the algae in the two localities are nearly the same but the strategies adopted for coming to terms with these conditions differ. The major compounds in the algae from Pirin are astaxanthin diacyl-glycosides whereas the Alps algae contain a prevalence of homologs of diacyl-astaxanthins. The third point is illustrated in Table 4, which clearly shows that, though the content of FAs and especially PUFAs in the two major classes of astaxanthin derivatives strongly differs, the unsaturation index is nearly identical and different PUFAs thus appear to have the same effect on the fluidity of cell membranes. We therefore assume that the algae from the three geographically very distant localities represent geographical varieties. Further analyses of field samples and experimental cultures are needed to elucidate whether these differences are caused by ecological factors or whether they can be associated with molecular identity of the strains. An important role in cell survival at low temperatures is played by unsaturation of fatty acids.

4. Experimental

4.1. Plant material

Red snow was aseptically collected on June 10th 2007 from surface layers of a snow field in the Lechtal Alps (Tirol, Austria). The sampling site was situated in the alpine zone of the Alperschönbachtal valley near the lake Knappenbödensee at an altitude of approximately 2350 m a.s.l. (47°11′02″N, 10°24′49″E). The sampling of red snow in the Pirin Mountains (Bulgaria) has been described in detail in Rezanka et al. (2008); briefly, red snow was aseptically collected on July 28th, 2006 from surface layers of a snow field in the Pirin Mountains (south western Bulgaria). The sampling site was situated in the alpine zone near the lake Tevno ezero at an altitude of 2546 m a.s.l. (41°41′93″N, 23°29′15″E). The third sample was collected on July 1st 2012 in the High Tatra Mountains (Slovak Republic). Red snow was sampled on the surface of ice cover of the lake Ľadové pleso, located in the Velká Studená dolina valley (49°18′41″N, 20°16′29″E, altitude 2057 m a.s.l.). The snow cover at all sites is seasonal. Snow samples were transported to the laboratory in a thermos bottle, identified under a light microscope, and the algal biomass was kept frozen until further analysis. The red blooms were formed entirely by spherical

cysts of *C. nivalis* (Bauer) Wille, and no flagellate stages were observed in the samples.

4.2. Standards, instrumentation, and isolation

Standard of astaxanthin diglucoside diester (18:1-G-A-G-18:1, i.e. di-[(6-*O*-oleoyl-β-D-glucopyranosyl)oxy]-astaxanthin) was prepared as described by Rezanka et al. (2008). All solvents were double distilled and degassed before use. All chemicals were obtained from Sigma–Aldrich, Prague.

Circular dichroism (CD) measurement was carried out under dry N_2 on a Jasco-500A spectropolarimeter at 24 °C.

Carotenoids were extracted with MeOH several times from the wet cell pellets (ca. 5 g) using an ultrasonicator for several seconds. The extract was partitioned with CH_2Cl_2 and H_2O, and then the CH_2Cl_2 layer was evaporated. All procedures were performed under dim light and argon.

The astaxanthin esters were saponified in 10% KOH–MeOH at room temperature overnight. A fatty acid fraction obtained from saponification was partitioned between alkali solution (pH 9) and Et_2O to remove basic and neutral components. The aqueous phase, containing fatty acids, was acidified to pH 2 and extracted with hexane. The fatty acid fraction was methylated using CH_2N_2. GC–MS of a FAME mixture was done on a Finnigan 1020 B in EI mode. Splitless injection was at 100 °C, and a fused silica capillary column (Supelcowax 10; 60 m × 0.25 mm i.d., 0.25 mm film thickness; Supelco, Prague) was used. The temperature program was as follows: 100 °C for 1 min, subsequently increasing at 20 °C/min to 180 °C and at 2 °C/min to 280 °C, which was maintained for 1 min. The carrier gas was helium at a linear velocity of 60 cm/s. All spectra were scanned within the range *m/z* 70–500. The structures of fatty acids were confirmed by comparison of retention times (Dembitsky et al., 1992a,b) and fragmentation patterns with those of the standard fatty acid methyl esters (Supelco, Prague).

For establishing the optical isomers of astaxanthin in the algae, the total extract was subjected to methanolysis in 0.5 ml of 0.1 M methanolic HCl at room temperature overnight, the reaction mixture was neutralized by $NaHCO_3$ solution and the solvent was removed under Ar gas.

4.3. Chiral HPLC

Analytical apparatus Sigma 3B (Perkin–Elmer, Norwalk, CT, USA) with an analytical column CHIRALCEL(R) OD-RH 150 mm × 2.1 mm × 5 μm (Merck Prague, Czech Republic). After injection of 100 μl of solution of total crude hydrolysate (5 mg/ml), separation was carried out by a mixture of acetonitrile/phosphoric acid (3.5 mM) at a flow rate of 0.5 ml/min under isocratic conditions and a temperature of 25 °C. Identification of astaxanthin peaks was achieved by using the wavelength of 470 nm. The CD spectra were measured in CH_2Cl_2 by means of a Jasco instrument (Jasco, Japan); see our previous paper (Rezanka and Dembitsky, 1998).

4.4. Preparative HPLC

The liquid chromatograph was the semipreparative Gradient LC System G-1 (Shimadzu, Kyoto, Japan) with two LC-6A pumps (0.5 ml/min), an SCL-6A system controller, an SPD ultraviolet detector, an SIL-1A sample injector and a C-R3A data processor, with preparative column Supelcosil LC-Si HPLC column 5 μm particle size, 25 cm length × 21.2 mm i.d. UV–vis detection at 470 nm.

4.5. LC–MS/APCI

HPLC equipment consisted of a 1090 Win system, PV5 ternary pump and automatic injector (HP 1090 series, Agilent, USA) and two Hichrom columns HIRPB-250AM 250 × 2.1 mm ID, 5 μm particle size, in series. This setup provided us with a high-efficiency column – approximately 26,000 plates/250 mm. A quadrupole mass spectrometer system Navigator (Finnigan MAT, San Jose, CA, USA) was used for analysis. The instrument was fitted with an atmospheric-pressure chemical ionization source (vaporizer temperature 400 °C, capillary heater temperature 250 °C, corona current 6 μA, sheath gas – high-purity nitrogen, pressure 0.4 MPa, and auxiliary gas (also nitrogen) flow rate 17 ml/min). Positively charged ions with *m/z* 100–1700 were scanned with a scan time of 0.5 s. The whole HPLC flow (0.4 ml/min) was introduced into the APCI source without any splitting. Astaxanthin derivatives were separated using a gradient solvent program with acetonitrile (ACN), dichloromethane (DCM) and methanol (MeOH), initial composition 50:25:25 (vol/vol/vol); linear from 8 to 55 min 25:25:50 (vol/vol/vol); held until 1 h; the composition was returned to the initial conditions over 5 min. A peak threshold of 0.05% intensity was applied to the mass spectra. Data acquisition and analyses were performed using PC with MassLab 2.0 for Windows XP applications/operating software.

4.6. HRMS/ESI

LTQ Orbitrap Velos (Thermo Scientific), a high resolution hybrid mass spectrometer was used. ESI–MS analysis was performed in the positive ion mode. MS spectra were obtained by the FT mode. MS spectra were acquired with target mass resolution of R = 30,000 at *m/z* 400. The ion spray voltage was set at 3500 V and the scan range of the instruments was set at *m/z* 150–1000. Nitrogen was used as a nebulizer gas – set at 18 arbitrary units (sheath gas) and 7 arbitrary units (aux gas). Helium was used as a collision gas for CID experiments. The CID normalization energy of 35% was used for the parent ions fragmentation. The MS/MS product ions were detected by the high resolution FT mode.

Flow Injection Analysis (FIA) was used for sample introduction into the heated ESI (H-ESI) ion source. Acetonitrile/water (50/50 v/v) was used at the flow rate of 150 μl/min. The H-ESI temperature was set to 250 °C.

4.7. ^1H NMR

The ^1H NMR spectrum of a mixture of optical isomers of all-trans astaxanthin was measured according to our previous paper (Rezanka and Dembitsky, 1998). Briefly, ^1H NMR spectrum was recorded with a Bruker AM 500 pulsed Fourier transform spectrometer (Karlsruhe, Germany) operating at 500 MHz for ^1H at ambient temperature.

Acknowledgments

The research was supported by the project GACR P503/11/0215 and by the Institutional Internal Projects RVO61388971 and RVO 67985939.

Appendix A. Supplementary data

Supplementary data associated with this article can be found, in the online version, at http://dx.doi.org/10.1016/j.phytochem.2013.01.003.

References

Abu-Lafi, S., Turujman, S.A., 1999. Reproducibility of the separation of astaxanthin stereoisomers on Pirkle covalent L-leucine and D-phenylglycine columns. J. Chromatogr. A 855, 157–170.

Andrenes, A.G., Starr, M.P., 1976. (3*R*,3′*R*)-Astaxanthin from yeast *Phaffia rhodozyma*. Phytochemistry 15, 1009–1011.

Andrenes, A.G., Phaff, H.J., Starr, M.P., 1976. Carotenoids of *Phaffia rhodozyma*, a red pigmented fermenting yeast. Phytochemistry 15, 1003–1007.

Bidigare, R.R., Ondrusek, M.E., Iturriaga, R., Harvey, H.R., Hoham, R.W., Macko, S.A., 1993. Evidence for a photoprotective function for secondary carotenoids of snow algae. J. Phycol. 29, 427–434.

Bonen, J., Soutar, C., Sernata, R.D., Lagocki, S., Nhite, D.A., Davies, S.J., Young, A.J., 2002. Utilization of (3*S*,3′*S*)-astaxanthin acyl esters in pigmentation of rainbow trout (*Oncorhynchus mykiss*). Aquac. Nutr. 8, 59–68.

Boussiba, S., 2000. Carotenogenesis in the green alga *Haematococcus pluvialis*, cellular physiology and stress response. Physiol. Plant. 108, 111–117.

Breithaupt, D.E., 2004. Identification and quantification of astaxanthin esters in shrimp (*Pandalus borealis*) and in a microalga (*Haematococcus pluvialis*) by liquid chromatography mass spectrometry using negative ion atmospheric pressure chemical ionization. J. Agric. Food Chem. 52, 3870–3875.

Breithaupt, D.E., Wirt, U., Bamedi, A., 2002. Differentiation between lutein monoester regioisomers and detection of lutein diesters from marigold flowers (*Tagetes erecta* L.) and several fruits by liquid chromatography–mass spectrometry. J. Agric. Food Chem. 50, 66–70.

Burgess, M.L., Barrow, K.D., Gao, C.X., Heard, G.M., Glenn, D., 1999. Carotenoid glycoside esters from the thermophilic bacterium *Meiothermus rubber*. J. Nat. Prod. 62, 859–863.

Coral-Hinostroza, G.N., Bjerkeng, B., 2002. Astaxanthin from the red crab langostilla (*Pleuroncodes planipes*): Optical *R*/*S* isomers and fatty acid moieties of astaxanthin esters. Comp. Biochem. Physiol. B 133, 437–444.

Dembitsky, V.M., Rezanka, T., Bychek, I.A., 1992a. Fatty-acids and phospholipids from lichens of the order Lecanorales. Phytochemistry 31, 851–853.

Dembitsky, V.M., Rezanka, T., Bychek, I.A., Shustov, M.V., 1992b. Fatty-acid composition of *Parmelia* lichens. Phytochemistry 31, 841–843.

Dodds, E.D., McCoy, M.R., Rea, L.D., Kennish, J.M., 2005. Gas chromatographic quantification of fatty acid methyl esters: Flame ionization detection vs. electron impact mass spectrometry. Lipids 40, 419–428.

Droop, M.R., 1955. Carotenogenesis in *Haematococcus pluvialis*. Nature 175, 42.

Frassanito, R., Cantonati, M., Tardio, M., Mancini, I., Guella, G., 2005. On-line identification of secondary metabolites in freshwater microalgae and cyanobacteria by combined liquid chromatography–photodiode array detection–mass spectrometric techniques. J. Chromatogr. A 1082, 33–42.

Frassanito, R., Flaim, G., Mancini, I., Guella, G., 2006. High production of unexpected carotenoids in Dinophyceae. Astaxanthin esters from the freshwater dinoflagellate *Tovellia sanguinea*. Biochem. Syst. Ecol. 34, 843–853.

Fujii, M., Takano, Y., Kojima, H., Hoshino, T., Tanaka, R., Fukui, M., 2010. Microbial community structure, pigment composition and nitrogen source of red snow in Antarctica. Microb. Ecol. 59, 466–475.

Giuffrida, D., La Torre, L., Manuela, S., Pellicano, T.M., Dugo, G., 2006. Application of HPLC–APCI–MS with a C-30 reversed phase column for the characterization of carotenoid esters in mandarin essential oil. Flavour Fragr. J. 21, 319–323.

Goodwin, T.W. (Ed.), 1980. The Biochemistry of Carotenoids. Plants. Chapman and Hall, New York.

Gorton, H.L., Vogelman, T.C., 2003. Ultraviolet radiation and the snow alga *Chlamydomonas nivalis* (Bauer) Wille. Photochem. Photobiol. 77, 608–615.

Gorton, H.L., Williams, W.E., Vogelman, T.C., 2001. The light environment and cellular optics of the snow alga *Chlamydomonas nivalis* (Bauer) Wille. Photochem. Photobiol. 73, 611–620.

Grewe, C., Menge, S., Griehl, C., 2007. Enantioselective separation of all-*E*-astaxanthin and its determination in microbial sources. J. Chromatogr. A 1166, 97–100.

Grung, M., Liaaen-Jensen, S., 1993. Algal carotenoids 52; secondary carotenoids of algae 3; carotenoids in a natural bloom of *Euglena sanguinea*. Biochem. Syst. Ecol. 21, 757–763.

Hoham, R.W., 1992. Environmental influences on snow algal microbes. In: Shafer, B. (Ed.), Proceedings of the Sixtieth Annual Western Snow Conference, Jackson, Wyoming, USA, April 14–16, 1992. pp. 78–83.

Hoham, R.W., Duval, B., 2001. Microbial ecology of snow and freshwater ice. In: Jones, H.G., Pomeroy, J.W., Walker, D.A., Hoham, R.W. (Eds.), Snow Ecology: An Interdisciplinary Examination of Snow-covered Ecosystems. Cambridge University Press, Cambridge, pp. 168–228.

Kobayashi, M., Okada, T., 2000. Protective role of astaxanthin against UV-B irradiation in the green alga *Haematococcus pluvialis*. Biotechnol. Lett. 22, 177–181.

Ling, H.U., 1996. Snow algae of the Windmill Islands region, Antarctica. Hydrobiologia 336, 99–106.

Lissitsyna, K., Huertas, S., Morales, R., Quintero, L.C., Polo, L.M., 2012. Determination of trace levels of fatty acid methyl esters in aviation fuel by GC × GC–FID and comparison with the reference GC–MS method. Chromatographia 75, 1319–1325.

Lorenz, R.T., Cysensky, G.R., 2000. Commercial potential for *Haematococcus* microalgae as natural source of astaxanthin. Trends Biotechnol. 18, 160–167.

Maoka, T., Komori, T., Matsuno, T., 1985. Direct diastereomeric resolution of carotenoids. 1. 3-Hydroxy-4-oxo β-end group. J. Chromatogr. 318, 122–124.

Megdal, P.A., Craft, N.A., Handelman, G.J., 2009. A simplified method to distinguish farmed (*Salmo salar*) from wild salmon: Fatty acid ratios versus astaxanthin chiral isomers. Lipids 44, 569–576.

Miao, F.P., Lu, D.Y., Li, Y.G., Zeng, M.T., 2006. Characterization of astaxanthin esters in *Haematococcus pluvialis* by liquid chromatography–atmospheric pressure chemical ionization mass spectrometry. Anal. Biochem. 352, 176–181.

Moretti, V.M., Mentasti, T., Bellagamba, F., Luzzana, U., Caprino, F., Turchini, G.M., Giani, I., Valfre, F., 2006. Determination of astaxanthin stereoisomers and colour attributes in flesh of rainbow trout (*Oncorhynchus mykiss*) as a tool to distinguish the dietary pigmentation source. Food Addit. Contam. 23, 1056–1063.

Muller, R.K., Bernhard, K., Mayer, H., Ruttimann, A., Vecchi, M., 1980. Contribution to the analytical separation and the synthesis of 3-hydroxy-4-oxocarotenoids. Helv. Chim. Acta 63, 1654–1664.

Muller, T., Bleiss, W., Martin, C.D., Rogaschewski, S., Fuhr, G., 1998. Snow algae from northwest Svalbard: Their identification, distribution, pigment and nutrient content. Polar Biol. 20, 14–32.

Ourisson, G., Rohmer, M., Poralla, K., 1987. Prokaryotic hopanoid and other polyterpenoid sterol surrogates. Annu. Rev. Microbiol. 41, 301–333.

Remias, D., Lutz-Meindl, U., Lutz, C., 2005. Photosynthesis, pigments and ultrastructure of the alpine snow alga *Chlamydomonas nivalis*. Eur. J. Phycol. 40, 259–268.

Remias, D., Karsten, U., Lutz, C., Leya, T., 2010. Physiological and morphological processes in the Alpine snow alga *Chloromonas nivalis* (Chlorophyceae) during cyst formation. Protoplasma 243, 73–86.

Renstrom, B., Berger, H., Liaaen-Jensen, S., 1981a. Natural occurrence of enantiomeric and *meso*-astaxanthin. 7. Esterified, optically pure (3*S*,3′*S*)-astaxanthin from flowers of *Adonis annua*. Biochem. Syst. Ecol. 9, 249–250.

Renstrom, B., Borch, G., LiaaenJensen, S., 1981b. Natural occurrence of enantiomeric and *meso*-astaxanthin. 4. Ex shrimps (*Pandalus borealis*). Comp. Biochem. Physiol. B 69, 621–624.

Renstrom, B., Borch, G., Skulberg, O.M., LiaaenJensen, S., 1981c. Natural occurrence of enantiometric and meso-astaxanthin. 3. Optical purity of (3*S*,3′*S*)-astaxanthin from *Haematococcus pluvialis*. Phytochemistry 20, 2561–2564.

Rezanka, T., Dembitsky, V.M., 1998. Chiral high performance liquid chromatography of astaxanthin's stereoisomers. Trends Comp. Biochem. Physiol. 5, 301–304.

Rezanka, T., Nedbalova, L., Sigler, K., Cepak, V., 2008. Identification of novel astaxanthin diglucoside diesters from snow alga *Chlamydomonas nivalis* by liquid chromatography–atmospheric pressure chemical ionization mass spectrometry. Phytochemistry 69, 479–490.

Rezanka, T., Olsovska, J., Sobotka, M., Sigler, K., 2009. The use of APCI–MS with HPLC and other separation techniques for identification of carotenoids and related compounds. Curr. Anal. Chem. 5, 1–25.

Rivera, S.M., Canela-Garayoa, R., 2012. Analytical tools for the analysis of carotenoids in diverse materials. J. Chromatogr. A 1224, 1–10.

Ronneberg, H., Renstrom, B., Aareskjold, K., LiaaenJensen, S., Vecchi, M., Leuenberger, F.J., Muller, R.K., Mayer, H., 1980. Natural occurrence of enantiomeric and *meso*-astaxanthin. 1. Ex lobster eggs (*Homarus gammarus*). Helv. Chim. Acta 63, 711–715.

Schweiggert, U., Kammerer, D.R., Carle, R., Schieber, A., 2005. Characterization of carotenoids and carotenoid esters in red pepper pods (*Capsicum annuum* L.) by high-performance liquid chromatography/atmospheric pressure chemical ionization mass spectrometry. Rapid Commun. Mass Spectrom. 19, 2617–2628.

Takaichi, S., Matsui, K., Nakamura, M., Muramatsu, M., Hanada, S., 2003. Fatty acids of astaxanthin esters in krill determined by mild mass spectrometry. Comp. Biochem. Physiol. B 136, 317–322.

Tinkler, J.H., Böhm, F., Schalch, W., Truscott, T.G., 1994. Dietary carotenoids protect human cells from damage. J. Photochem. Photobiol. B: Biol. 26, 283–285.

Turujman, S.A., 1993. Rapid direct resolution of the stereoisomers of all-trans astaxanthin on a Pirkle covalent L-leucine column. J. Chromatogr. 631, 197–199.

Vecchi, M., Muller, R., 1979. Separation of (3*S*,3′*S*)-, (3*R*,3′*R*)- and (3*S*,3′*R*)-astaxanthin via (−)-camphanic acid esters. J. High Resolut. Chromatogr. Chromatogr. Commun. 2, 195–196.

Yamano, Y., Sakai, Y., Hara, M., Ito, M., 2002. Carotenoids and related polyenes. Part 9. Total synthesis of thermozeaxanthin and thermocryptoxanthin and the stabilizing effect of thermozeaxanthin on liposomes. J. Chem. Soc. Perkin Trans. I, 2006–2013.

Yokoyama, A., Adachi, K., Shizuri, Y., 1995a. New carotenoid glucosides, astaxanthin glucoside and adonixanthin glucoside, isolated from the astaxanthin-producing marine bacterium, *Agrobacterium aurantiacum*. J. Nat. Prod. 58, 1929–1933.

Yokoyama, A., Sandmann, G., Hoshino, T., Adachi, K., Sakai, M., Shizuri, Y., 1995b. Thermozeaxanthins, new carotenoid–glycoside–esters from thermophilic eubacterium *Thermus thermophilus*. Tetrahedron Lett. 36, 4901–4904.

Yokoyama, A., Shizuri, Y., Hoshino, T., Sandmann, G., 1996. Thermocryptoxanthins: Novel intermediates in the carotenoid biosynthetic pathway of *Thermus thermophilus*. Arch. Microbiol. 165, 342–345.

Yokoyama, A., Shizuri, Y., Misawa, N., 1998. Production of new carotenoids, astaxanthin glucosides, by *Escherichia coli* transformants carrying carotenoid biosynthetic genes. Tetrahedron Lett. 39, 3709–3712.

Yuan, J.P., Chen, F., Liu, X., Li, X.Z., 2002. Carotenoid composition in the green microalga *Chlorococcum*. Food Chem. 76, 319–325.